Zhang *et al. J Wireless Com Network* (2023) 2023:64
https://doi.org/10.1186/s13638-023-02264-1

EURASIP Journal on Wireless Communications and Networking

RESEARCH Open Access

Joint resource allocation and user association for multi-cell integrated sensing and communication systems

Jiahui Zhang[1], Zesong Fei[1], Xinyi Wang[1], Peng Liu[1], Jingxuan Huang[1*] and Zhong Zheng[1]

*Correspondence:
jxhbit@gmail.com

[1] School of Information and Electronics, Beijing Institute of Technology, Beijing, China

Abstract

The densification of the orthogonal frequency division multiplexing (OFDM) based fifth-generation communication systems, as well as the requirement of integrating sensing and communication functionalities, has promoted the development of integrated-sensing-and-communication (ISAC) dense cellular networks (DCNs). In the OFDM-based ISAC-DCN, multiple base stations simultaneously serve mobile users and sense targets based on the echo of downlink communication signals. In this paper, we establish the interference model in ISAC-DCN for sensing and communication. Focusing on the interference management of the ISAC-DCN, we investigate the multi-dimension resource allocation problem. In particular, we aim to maximize the network utility by jointly optimizing sub-band allocation, user association, and transmission power under the sensing signal-to-interference-plus-noise ratio constraint to be solved iteratively. The mixed-integer optimization problem is decoupled into three sub-problems. Specifically, a greedy genetic sub-band allocation scheme is proposed for sub-band allocation to reduce total interference. We employ the successive convex approximation technique to transform the transmission power control sub-problem and solve it via geometric programming. Simulation results illustrate the trade-off between sensing and communication performances, and show that the proposed algorithm significantly improves the network utility and achieves higher detection probability.

Keywords: Integrated sensing and communication, Dense cellular network, Resource allocation, User association

1 Introduction

Integrated sensing and communication (ISAC) has been one of the research hotspots, due to its potential to reduce hardware costs and improve spectral efficiency. Researchers have been devoting their efforts to promoting the realization of ISAC technique [1]. As the waveform adopted by the fifth-generation (5 G) new radio (NR) [2], the orthogonal frequency division multiplexing (OFDM) waveform has been used widely in modern communication systems, while it also has an excellent ambiguity function, which promotes its application in sensing [3–5]. Therefore, developing ISAC techniques based on

OFDM waveform can simultaneously satisfy the communication requirement and provide sensing functionality with little change on the existing 5 G systems.

Motivated by the aforementioned advantages, some works have investigated ISAC design in the framework of 5 G NR systems [5–10]. In [5], the self-ambiguity and cross-ambiguity functions of several synchronization signals and reference signals (RSs) in OFDM waveform were analyzed. In [6], RSs used for channel estimation in OFDM waveform were multiplexed as sensing signal. Considering the energy efficiency, RS density and power allocation between pilots and data symbols were optimized to minimize the total transmission power, while satisfying the communication and radar sensing requirements. In [7], the 5 G network was utilised to serve as the illumination source for passive bi-static radar to detect the target, which verifies the possibility of 5 G-based passive bi-static radar. In [8], the base station (BS) was deployed as a monostatic sensor to estimate the targets' ranges, speeds, and directions of arrival (DoAs) via beam scanning. The targets' positions were then obtained based on the estimated ranges and DoAs. However, single-station based sensing faces several problems, e.g., sensing blind areas, limited detection range, and poor robustness. To address this issue, in [9], the authors proposed a novel two-phase framework for device-free sensing in an OFDM cellular network to achieve ISAC, in which adjacent BSs are assigned orthogonal sub-bands to avoid significant inter-cell interference. A maximum-likelihood based algorithm was provided to deal with the target association issue to achieve multi-BS cooperative sensing. Besides, based on the 5 G NR standard framework configuration, the authors in [10] proposed a staggered framework structure for ISAC cellular network to avoid self-interference and realize the parallelism of sensing units and communication cells. However, in this scheme, discontinuous OFDM symbols used for sensing will reduce the speed measurement accuracy due to the reduction of coherent accumulation time.

Although the promising dense cellular networks (DCNs) significantly promote the capacity of wireless communication systems [11], as well as more robust and accurate sensing through multi-BS cooperation. However, higher frequency reuse among different BSs results in much higher inter-cell interference (ICI), thereby degrading the performance of both communication and sensing functionalities. Facing this issue, there have been a lot of researches [12–20] on suppressing the ICI caused by FR in cellular networks. In general, physical separation-based frequency assignment and transmission power control are two underlying concepts for ICI mitigation [12]. Since the frequency assignment problem is an NP problem, metaheuristic algorithms such as Ant Colony Optimization [13], Differential Evolution [14] and Greedy algorithm [15], as well as branch-and-bound algorithm [16] were used to effectively solve this problem. In [17], the quality of service under various FR schemes, including partial FR, fractional frequency FR and soft FR, etc., were analyzed. In [18], the authors investigated joint sub-band and power allocation to improve inter-cell fairness in femtocell OFDM networks. Moreover, since users are distributed unevenly among cells, the load of BSs is imbalanced, which also leads to the degradation of system communication performance. Therefore, in [15] and [19], (partial) FR and user association schemes were jointly optimized to maximize the network utility or system throughput. In [20], the authors presented a load-aware and self-adapting frequency allocation scheme to cope with the changing traffic conditions.

However, the aforementioned studies only focused on improving communication performance, such as throughput, quality of service, and network utility, while the impact of interference on sensing still needs to be addressed. In [16], the authors studied the sensing interference management in multiple UAV networks through joint channel allocation and power control but did not consider the communication performance. In [21], the authors studied the issue of power control for cooperative ISAC networks under the sensing signal-to-interference-plus-noise (SINR) constraint, where the Lagrangian method was employed. Thus, in this paper, we aim to address the interference management of the OFDM-based ISAC-DCN via joint resource allocation and user association. In particular, both sensing and communication performances are taken into consideration. For communication performance, we adopt the network utility metric [22], which considers both sum-rate and fairness among different users. For sensing performance, to improve the target detection probability, which is directly determined by the SINR of the received echo signals [23], we adopt the SINR of the echo signal received at each BS as the metric.

The main contributions of this paper are summarized as follows.

(1) The interference models caused by FR in ISAC-DCN are analyzed from the perspectives of both communication and sensing. Thereafter, a joint resource allocation and user association problem is formulated with the aim of maximizing the network utility of the ISAC-DCN under both sensing signal-to-interference-plus-noise (SINR) and transmit power constraints.
(2) The formulated highly non-convex problem is decomposed into three sub-problems, i.e., sub-band allocation, user association, and transmission power control sub-problems, and an alternating optimization based algorithm is proposed to solve the original problem by iteratively solving the three sub-problems. In particular, a greedy genetic algorithm (GRGA) is proposed to solve the sub-band sub-problem, while the Hungarian algorithm and successive convex approximation (SCA) technique are utilized to solve the sub-problems of user association and transmission power control, respectively.
(3) The effectiveness of the proposed algorithm in improving the network utility and detection probability is verified through numerical simulation. Compared with both conventional and state-of-the-art schemes, the proposed algorithm is able to significantly improve both network utility and detection probability. Moreover, the trade-off between communication and sensing performances is also illustrated.

The rest of this paper is organized as follows. In Sect. 2, we introduce both system models and interference models of ISAC-DCN. Then, we formulate a problem of joint sub-band allocation, user association, and transmission power control in Sect. 3. The algorithm for solving the problem is presented in Sect. 4. Then we present the numerical simulation results as well as discussions in Sect. 5. Finally, we conclude the paper in Sect. 6.

The notations used in this paper are as follows. Lower case normal letters a denote scalars, lower-case bold letters $\mathbf{a}$ denote column vectors and upper-case bold characters $\mathbf{A}$ denote matrices. $(\cdot)^T$ represents the transpose.

2 System model

In this section, we first describe the OFDM based ISAC-DCN model, where multiple BSs simultaneously provide communication services to mobile users, and at the same time sense the targets based on the echo of DL communication signals. Subsequently, we introduce the interference models for both communication and sensing.

2.1 System description

We consider an OFDM based ISAC-DCN as shown in Fig. 1a, which consists of M BSs, denoted by $\mathcal{M} = \{1, \ldots, M\}$, N $(N > M)$ mobile users, denoted by $\mathcal{N} = \{1, \ldots, N\}$, and T targets, denoted by $\mathcal{T} = \{1, \ldots, T\}$. Due to the scarcity of spectral resource, we assume only K $(K < N)$ orthogonal sub-bands are available, which are denoted by $\mathcal{K} = \{1, \ldots, K\}$. The bandwidth of each sub-band is denoted by B. The transmission power of the BSs are denoted as $\mathbf{p} = [p_1, \ldots, p_M]$, where the ith element represents the power of the ith BS. In addition, a central station is deployed and connected to all BSs to perform resource allocation and signal processing [9].

The detailed signal transmission, reflection and interference are illustrated in Fig. 1b. The BSs provide communication services for users via OFDM signal in DL time slots. In a meantime, the DL communication signals are reflected by the targets and received by the BSs, based on which the ISAC-DCN can cooperatively estimate the targets' locations [8] as well as velocities. The BSs marked with the same color are assigned the same sub-band. Such frequency multiplexing between BSs introduces interference to both communication and sensing.

Furthermore, we make the following assumptions for the remainder of this paper:

- Each BS occupies one sub-band. $w_{k,i} = 1$ denotes BS i is assigned with sub-band k and 0 otherwise, and $\sum_{k=1}^{K} w_{k,i} = 1, \forall i \in \mathcal{M}$.
- Each user is associated with one base station. $u_{i,n} = 1$ denotes user n is associated with BS i and 0 otherwise, and $\sum_{i=1}^{M} u_{i,n} = 1, \forall n \in \mathcal{N}$.
- Each BS only focuses on the sensing results within a predetermined sensing range to improve the accuracy of cooperative sensing and reduce the appearance of ghost tar-

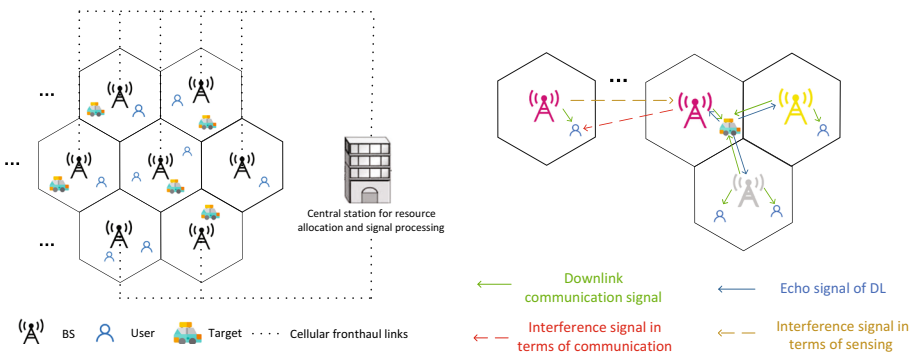

Fig. 1 **a** An illustration of the considered OFDM based ISAC-DCN Model. **b** Details of signal transmission, reflection and interference

gets. In other words, the target appearing in a certain area is sensed by specific BSs. The sensing range of each BS is set as R.

2.2 Communication interference model

The time-domain signal in one OFDM symbol period transmitted by the ith BS is given by

$$\mathbf{x_i} = \sqrt{p_i}\left[x_{i,L-Q+1}, \ldots, x_{i,L}, x_{i,1}, \ldots, x_{i,L}\right]^T, \ \forall i \in \mathcal{M}, \tag{1}$$

where L denotes the IFFT size in OFDM modulation, and Q denotes the length of the cyclic prefix (CP).

The received signal at the nth user associated with the ith BS in the lth OFDM sample period is expressed as

$$y_{c_{i,n},l} = h_{i,n}x_{i,l} + \sum_{\forall i \in \mathcal{M}, j \neq i} \mathbf{w}_i^T \mathbf{w}_j h_{j,n} x_{j,l} + z_n, \ \forall j \in \mathcal{M}, \forall n \in \mathcal{N}, \tag{2}$$

where $h_{i,n}$ denotes the DL communication channel from the ith BS to the nth user, $w_{k,i} \in \{0, 1\}$, and $z_n \sim \mathcal{N}(0, \sigma^2)$ denotes additive white Gaussian noise (AWGN) at the nth user. In addition, $h_{i,n}$ considers both the small-scale Rayleigh fading effect and path loss effect, and time domain expression is given by

$$h_{i,n}(t) = f_{i,n}\sqrt{\rho_0 d_{i,n}^{-2}}\delta(t - \tau_{i,n}) \tag{3}$$

in which $f_{i,n}$ is a Rayleigh random variable with zero mean and variance σ_r^2, ρ_0 denotes the path loss at the reference distance $d_0 = 1$ m, $d_{i,n}$ denotes the distance between BS i and user n, and $\tau_{i,n} = d_{i,n}/c$, with c being the speed of light.

Therefore, the SINR of the received signal at the nth user in the lth OFDM sample period is expressed as [24]

$$\gamma_{c_{i,n}} = \frac{\left|h_{i,n}x_{i,l}\right|^2}{\sum\limits_{\forall j \in \mathcal{M}, j \neq i} \left|\mathbf{w}_i^T \mathbf{w}_j h_{j,n} x_{j,l}\right|^2 + \sigma^2}, \ \forall i, j \in \mathcal{M}, \forall n \in \mathcal{N}, \tag{4}$$

Under static channels and flat transmission power spectral density, the optimal frequency allocation for one BS is equal allocation among its associated users [22]. Therefore, we assume that each user served by the same BS is assigned equal bandwidth. The bandwidth occupied by the user associated with the ith BS is expressed as

$$B_{i,n} = \frac{B}{\sum\limits_{n \in \mathcal{N}} u_{i,n}}, \forall i \in \mathcal{M}, \tag{5}$$

where $u_{i,n} \in \{0, 1\}$.

The data rate of user n associated with BS i is express as

$$C_{i,n} = B_{i,n}\log\left(1 + \gamma_{c_{i,n}}\right), \forall i \in \mathcal{M}, \forall n \in \mathcal{N}, \tag{6}$$

which is determined by γ_{c_i} and $B_{i,n}$. According to (4), the communication SINR γ_{c_i}, is related to sub-band allocation, user association and transmission power. Moreover, $B_{i,n}$, is related to the number of users served by BS i. Therefore, in this paper, we aim at reducing the co-channel interference and increasing the data rate through resource allocation, including sub-band and transmission power, as well as user association.

2.3 Sensing interference model

The echo signal received by the receive antenna of the ith BS is expressed as

$$y_{s_i} = \sum_{t=1}^{T}\sum_{j=1}^{M} h_{j,t,i}x_{j,l} + \sum_{\forall j\in\mathcal{M}, j\neq i} \mathbf{w}_i^T\mathbf{w}_j h_{j,i}x_{j,l} + z_i,\ \forall i,j\in\mathcal{M}, \tag{7}$$

where $h_{j,i}$ and $h_{j,t,i}$, respectively, denotes the complex channel of "BS j-BS i" and "BS j-target t-BS i", and $z_i \sim \mathcal{N}(0,\sigma^2)$ denotes AWGN at the ith BS. The time domain expression of $h_{j,i}$ and $h_{j,t,i}$ is, respectively, given by

$$h_{j,i}(t) = f_{j,i}\sqrt{\rho_0 d_{j,t}^{-2}}\delta(t-\tau_{j,i}) \tag{8}$$

$$h_{j,t,i}(t) = \psi\sqrt{\rho_0 d_{j,t}^{-2}(4\pi d_{t,i})^{-2}}\exp(-2j\pi f_{d_{j,t,i}}t)\delta(t-\tau_{j,t,i}) \tag{9}$$

in which ψ denotes radar cross section (RCS), $\tau_{j,i} = d_{j,i}/c$, $\tau_{j,t,i} = (d_{j,t}+d_{t,i})/c$, and $f_{d_{j,t,i}} = (v_{t,j}+v_{t,i})f_c/c$, with $v_{t,j}$, $v_{t,i}$ and f_c denote the radial velocity of target t relative to BS j, the radial velocity of target t relative to BS i and the center carrier frequency, respectively.

In this paper, we mainly consider the direct interference among the BSs sharing the same sub-band, while the scattered interference is ignored due to its much lower power. In this case, (7) can be simplified as

$$y_{s_i} = \sum_{t=1}^{T} h_{i,t,i}x_{i,l} + \sum_{\forall j\in\mathcal{M}, j\neq i} \mathbf{w}_i^T\mathbf{w}_j h_{j,i}x_{j,l} + z_i,\ \forall i,j\in\mathcal{M}, \tag{10}$$

in which $\sum_{j=1}^{M}\mathbf{w}_i\mathbf{w}_j^H h_{j,i}x_{j,l}$ denotes the interference among the BSs sharing the same sub-band. By applying point-wise division [4] and two-dimensional DFT (2D-DFT), the BS i can eliminate the impact of the communication data symbols $x_{i,l}$ and obtain the distance and speed information[25].

Generally speaking, cooperative sensing can be realized in two ways. One way is to directly upload the signals received by each sensing node to the center for joint signal processing [26], while the other way is to upload the data local processing results of each node, based on which the center conducts further processing, e.g., target association [9]. The latter scheme benefits from lower processing complexity, and therefore is considered in this paper. In other words, the ISAC BSs are considered to firstly sense the targets in a separate way, and then upload the processing results to the center. In order to guarantee the performance of cooperative sensing, the sensing

performance of each node is required to satisfy a given threshold. Supposing the detection range of each BS is R, the SINR of the received echo signal is given by

$$\begin{aligned}\gamma_{s_i} &= \frac{\chi |h_{i,t_R,i} x_{i,l}|^2}{\beta \sum\limits_{\forall j \in \mathcal{M}, j \neq i} \left|\mathbf{w}_i^T \mathbf{w}_j h_{j,i} x_{j,l}\right|^2 + \sigma^2} = \frac{\chi |h_{i,t_R,i}|^2 p_i}{\beta \sum\limits_{\forall j \in \mathcal{M}, j \neq i} \left|\mathbf{w}_i^T \mathbf{w}_j h_{j,i}\right|^2 p_j + \sigma^2} \\ &= \frac{\chi (4\pi)^2 \psi^2 \rho_0 R^{-4} p_i}{\beta \sum\limits_{\forall j \in \mathcal{M}, j \neq i} \mathbf{w}_i^T \mathbf{w}_j f_{j,i}^2 \rho_0^2 d_{j,i}^{-2} p_j + \sigma^2}\end{aligned} \tag{11}$$

where χ denotes the correlation gain of the transmitted symbols [25] and β denotes the suppression gain for the direct interference. As BSs can share transmission signals through backhaul connections and obtain delay information between BSs by channel estimation. Therefore, the direct interference in the received superimposed signals can be suppressed by the extended cancellation algorithm (ECA)[27], which operates by subtracting appropriately weighted delayed copies of the reference signal from the received signal.

Based on the Neyman-Pearson criterion, utilizing the Generalized Likelihood Ratio Test (GLRT), the asymptotic detection probability is given as [28]

$$P_D = 1 - \mathcal{F}_{\chi_2^2(\gamma_{s_i})}\left(\mathcal{F}_{\chi_2^2}^{-1}(1 - P_{FA})\right), \tag{12}$$

where P_{FA} is the false alarm probability of sensing, $\mathcal{F}_{\chi_2^2(\gamma_{s_i})}$ devotes the noncentral chi-squared distribution function with two degrees of freedom and noncentrality parameter and γ_{s_i}, $\mathcal{F}_{\chi_2^2}$ is the central chi-squared distribution function with two degrees of freedom, with $\mathcal{F}_{\chi_2^2}^{-1}$ being its inverse function. For given P_{FA}, the distribution of P_D follows noncentral chi-squared distribution function with two degrees of freedom and noncentrality parameter γ_{s_i}. As can be readily seen from (12), the detection probability P_D is positively correlated with SINR γ_{s_i} [28]. Therefore, we transform the detection probability metric into the SINR performance metric. According to (11), the SINR of the echo signal γ_{s_i} is related to sub-band allocation and transmission power. Appropriate sub-band allocation and transmission control can improve the sensing SINR, thereby improving the detection probability.

3 Problem formulation

In this section, we formulate the problem of joint sub-band allocation, user association, and transmission power control. To be specific, we consider to maximize the network utility under the constraints of the echo signal SINR threshold, which is formulated as follows.

$$\max_{\mathbf{p},\mathbf{w},\mathbf{u}} \quad \sum_{n=1}^{N} \log\left(\sum_{i=1}^{M} u_{i,n} C_{i,n}\right) \tag{13}$$

$$s.t. \quad \gamma_{s_i} \geq \Gamma, \tag{13a}$$

$$w_{k,i} \in \{0,1\}, \tag{13b}$$

$$\sum_{k=1}^{K} w_{k,i} = 1, \quad \forall i \in \mathcal{M}, \tag{13c}$$

$$u_{k,i} \in \{0,1\}, \tag{13d}$$

$$\sum_{i=1}^{M} u_{i,n} = 1, \forall n \in \mathcal{N}, \tag{13e}$$

$$p_{\min} \leq p_i \leq p_{\max}, \tag{13f}$$

where Γ in the constraint (13a) denotes the SINR threshold of echo signal for sensing, and the constraint (13f) limits the BS transmission power.

4 Proposed method

To deal with the non-convex and NP-hard problem (12), we decompose it into three sub-problems, i.e., sub-band allocation, user association, and transmission power control sub-problems.

4.1 Sub-band allocation

With the fixed transmission power $\mathbf{p}_0$ and user association strategy, the problem (13) can be simplified as the following sub-problem.

$$\begin{aligned} \max_{\mathbf{w}} \ & \sum_{n=1}^{N} \log\left(\sum_{i=1}^{M} u_{i,n} B_{i,n} \log\left(1+\gamma_{c_{i,n}}\right)\right) \\ s.t.\ & w_{k,i} \in \{0,1\}, \\ & \sum_{k=1}^{K} w_{k,i} = 1, \forall k \in \mathcal{K}, \forall i \in \mathcal{M}. \end{aligned} \tag{14}$$

The problem (14) is a 0–1 programming problem, and the objective function is non-convex even for continuous $\mathbf{w}$, which makes it challenging to solve. Nevertheless, notice that the network utility is mainly related to the SINR of each user with equal bandwidth allocation. Furthermore, with the transmission power fixed, according to (11), the SINR is only related to the inter-cell interference. Therefore, we propose to alternatively minimize the total inter-cell interference, which can be formulated as

$$\begin{aligned} \min_{\mathbf{w}} \ & \sum_{m=1}^{M} \sum_{j=1, j\neq i}^{M} \frac{p_j}{p_i} \left| \mathbf{w}_i^T \mathbf{w}_j h_{j,i} x_{j,l} \right|^2 \\ s.t.\ & w_{k,i} \in \{0,1\}, \\ & \sum_{k=1}^{K} w_{k,i} = 1, \forall k \in \mathcal{K}, \forall i \in \mathcal{M}. \end{aligned} \tag{15}$$

Since there are totally K^M different allocation schemes, it is extremely complex to solve the above sub-problem via exhaustive searching. Besides, the greedy channel allocation algorithm [29] and low-complexity branch-and-bound based channel allocation [16] may result in a locally optimal solution, thereby increasing inter-cell interference and degrading network utility and sensing performance. Motivated by the ability of the genetic algorithm [30] in increasing the possibility of finding the optimal global solution, we proposed the sub-band allocation scheme based on the greedy genetic idea that combines the greedy algorithm and genetic algorithm [31] to reduce complexity and improve the sensing and communication performance.

Firstly, we represent the sub-band allocation of each BS by K base coding. For example, when $M = 4$ and $K = 2$, coding mode '2112' means that BS 1, 2, 3, and 4 are assigned with sub-band 2, 1, 1, and 2, respectively. As the interference among different BSs to be addressed are dependent. Thus, we firstly pick K BSs in a greedy manner and assign them K different sub-bands, which avoids the uncertainty of weight due to dependence. Specifically, the two nearest BSs are selected and then the BS that is closest to the set of the selected BSs is selected one by one. The selected K BSs are assigned different sub-bands. Subsequently, for other BSs, we assign them sub-bands randomly, and generate Q_1 initial allocation schemes. The initial Q_1 allocation schemes are, respectively, represented by the above K base coding, and form Q_1 coding sequences. Unlike the one-to-one mapping in [28], the same sub-band can be repeatedly allocated. Correspondingly, we define the fitness function of each allocation scheme as

$$\mathcal{F} = \sum_{m=1}^{M} \sum_{j=1, j\neq i}^{M} \frac{p_j}{p_i} \left| \mathbf{w}_i^T \mathbf{w}_j h_{j,i} x_{j,l} \right|^2. \tag{16}$$

The smaller the value of $\mathcal{F}$ is, the greater the fitness of the scheme is. Based on the fitness value, we select Q_2 schemes to be retained, in which the scheme with high fitness value has a high probability of being retained. Finally, the coding sequences of schemes retained are crossed and mutated to generate new candidate schemes. The specific steps of the algorithm are summarized in Algorithm 1.

Algorithm 1 Greedy genetic channel allocation algorithm

1: Represent the sub-band allocation of each BS by K base coding.
2: Pick K BSs in a greedy manner and assign them K different sub-bands.
3: Allocate other BSs sub-bands randomly, and generate Q_1 initial allocation schemes.
4: **repeat**
5: Calculate the fitness of each allocation scheme based on (16).
6: Select Q_2 schemes to be retained based on fitness.
7: Crossover and mutate the reserved schemes with probability pr_c and pr_m respectively to generate new schemes.
8: **until** The maximum number of iterations is reached.
Output $\mathbf{w}^*$.

4.2 User association

With given sub-band allocation scheme and fixed transmission power, the user association sub-problem can be expressed as follows.

$$\begin{aligned}
&\max_{\mathbf{u}} \sum_{n=1}^{N} \log \left(\sum_{i=1}^{M} u_{i,n} \frac{B}{\sum_{n \in N} u_{i,n}} \log \left(1+\gamma_{c_{i,n}}\right) \right) \\
&s.t.\ u_{k,i} \in \{0,1\}, \\
&\quad \sum_{i=1}^{M} u_{i,n} = 1, \forall i \in \mathcal{M}, \forall n \in \mathcal{N},
\end{aligned} \tag{17}$$

where $u_{i,n} = 1$ means user n is associated with BS i and 0 otherwise. Note that for each n, only one $u_{i,n}$ for all n's is equal to 1, which means that the user can only be served by one BS. Therefore, for given sub-band allocation and transmission, the objective function of the problem (14) can be compactly and equivalently expressed as

$$\begin{aligned}
&\sum_{n=1}^{N} \log \left(\sum_{i=1}^{M} u_{i,n} \frac{B}{\sum_{n \in \mathcal{N}} u_{i,n}} s_{i,n} \right) \\
&\quad = \sum_{n=1}^{N} \sum_{i=1}^{M} u_{i,n} \log \left(\frac{B}{\sum_{n \in \mathcal{N}} u_{i,n}} s_{i,n} \right) \\
&\quad = \sum_{n=1}^{N} \sum_{i=1}^{M} u_{i,n} \log \left(B s_{i,n} \right) - \sum_{i=1}^{M} \left(\sum_{n=1}^{N} u_{i,n} \right) \log \left(\sum_{n \in \mathcal{N}} u_{i,n} \right)
\end{aligned} \tag{18}$$

By introducing $(N_b - 1)$ dummy BSs, the sum of several-to-one weight in (17, 18) can be transformed into the sum of one-to-one matching weight [32]. Thus, the above problem is equivalent to

$$\begin{aligned}
&\max_{\mathbf{u}} \sum_{n=1}^{N} \sum_{i=1}^{M} \sum_{q=1}^{N_b} u_{i,n}^{(q)} w_{i,n}^{(q)} \\
&s.t.\ u_{i,n}^{(q)} \in \{0,1\}, \\
&\quad \sum_{i=1}^{M} \sum_{q=1}^{N_b} u_{i,n}^{(q)} = 1, \forall n \in \mathcal{N}, \\
&\quad \sum_{n=1}^{N} u_{i,n}^{(q)} = 1, \forall i \in \mathcal{M}, \forall q = 1, \ldots, N_b, \\
&\quad w_{i,n}^{(1)} = \log \left(B s_{i,n} \right), \\
&\quad w_{i,n}^{(q)} = \log \left(B s_{i,n} \right) - q \log q + (q-1) \log (q-1), \forall q = 1, \ldots, N_b,
\end{aligned} \tag{19}$$

which is a bi-partite matching problem by setting $N_b = N$, and can be solved efficiently by the Hungarian algorithm, which has been proven superior to greedy and improved greedy algorithms for user association [33, 34].

4.3 Transmission power control

With given sub-band allocation scheme **w** and user association scheme **u**, the transmission power control sub-problem is expressed as follows.

$$\begin{aligned} &\max_{\mathbf{p}} \sum_{n=1}^{N} \log\left(\sum_{i=1}^{M} u_{i,n} B_{i,n} \log\left(1+\gamma_{c_{i,n}}\right)\right) \\ &s.t.\ \gamma_{s_i} \geq \Gamma, \\ &\quad p_{\min} \leq p_i \leq p_{\max}. \end{aligned} \tag{20}$$

Different from the power control based network utility maximization problem, the above problem cannot be solved via the conventional water-filling type of solution [35] due to the existence of the sensing SINR constraint. Meanwhile, due to the non-convexity of the objective function and constraints, problem (21) cannot be directly solved using CVX tools. Firstly, by introducing an auxiliary variable $\boldsymbol{\eta} = \{\eta_1, \cdots, \eta_N\}$, the sub-problem above can be reformulated as

$$\max_{\mathbf{p},\boldsymbol{\eta}} \sum_{n=1}^{N} \log\left(\eta_n\right) \tag{21}$$

$$s.t. \quad \gamma_{s_i} \geq \Gamma,\ \forall i \in \mathcal{M}, \tag{21a}$$

$$p_{\min} \leq p_i \leq p_{\max}, \tag{21b}$$

$$\eta_n \leq \sum_{i=1}^{M} u_{i,n} B_{i,n} \log\left(1+\gamma_{c_{i,n}}\right). \tag{21c}$$

However, problem (21) is still a non-convex optimization problem due to the non-convexity of constraint (21c). We employ SCA technique to address this issue. By applying the first-order Taylor series expansion at the given point $\widetilde{p}$, the constraint (21c) can be approximated as

$$\eta_n^{(a+1)} \leq \sum_{i=1}^{M} u_{i,n} B_{i,n} \left[\xi_{i,n}^{(a)} \log\left(\widetilde{\gamma}_{c_{i,n}}^{(a+1)}\right) + \varepsilon_{i,n}^{(a)}\right], \tag{22}$$

where $\xi_{i,n}^{(a)} = \frac{\widetilde{\gamma}_{u_{i,n}}^{(a)}}{1+\widetilde{\gamma}_{c_{i,n}}^{(a)}}$ and $\varepsilon_{i,n}^{(a)} = \log\left(1+\widetilde{\gamma}_{c_{i,n}}^{(a)}\right) - \xi_{i,n}^{(a)} \log\left(\widetilde{\gamma}_{u_{i,n}}^{(a)}\right)$, superscripts (a) and $(a+1)$ represent the ath and $(a+1)$th iteration, respectively.

Thereafter, the problem (21) can be transformed into the following form.

$$\max_{\mathbf{p}^{(a+1)},\boldsymbol{\eta}^{(a+1)}} \quad \sum_{n=1}^{N} \eta_n^{(a+1)} \tag{23}$$

$$s.t. \quad \gamma_{s_i} \geq \Gamma,\ \forall i \in M, \tag{23a}$$

$$p_{\min} \leq p_i \leq p_{\max}, \tag{23b}$$

$$\eta_n^{(a+1)} \leq \sum_{i=1}^{M} u_{i,n} B_{i,n} \left[\xi_{i,n}^{(a)} \log \left(\gamma_{s_i}^{(a+1)} \right) + \varepsilon_{i,n}^{(a)} \right], \tag{23c}$$

Theorem 1 *Problem* (23) *can be solved by geometric programming* (*GP*).

1 ***Proof***

It can be seen from (11) that constraint (20a) is a posynomial function of $\mathbf{p}$*. Next, we prove that constraint (20c) is convex [36]. Constraint (20c) can be expressed as,*

$$\begin{aligned} \eta_n^{(a+1)} &\leq \sum_{i=1}^{M} u_{i,n} B_{i,n} \left[\xi_{i,n}^{(a)} \log \left(\gamma_{s_i}^{(a+1)} \right) + \varepsilon_{i,n}^{(a)} \right] \\ &= \sum_{i=1}^{M} u_{i,n} B_{i,n} \xi_{i,n}^{(a)} \log \left(\chi |h_{i,t_R,i}|^2 p_i^{(a+1)} \right) \\ &- u_{i,n} B_{i,n} \log \left(\beta \sum_{j=1, j\neq i}^{M} \left| \mathbf{w}_i^T \mathbf{w}_j h_{j,i} \right|^2 p_j^{(a+1)} + \sigma^2 \right) \\ &+ u_{i,n} B_{i,n} \varepsilon_{i,n}^{(a)} \end{aligned} \tag{24}$$

which is convex due to the convexity of $\log(\cdot)$. The objective function of (22) and constraint (22b) are also convex. Therefore, the problem (22) is composed of posynomial function and convex functions, it can be solved by GP. □

Therefore, the transmission power control sub-problem (19, 20) can be solved by GP and successive convex approximation (SCA) technique.

Algorithm 2 Overall Algorithm for Solving Problem (13)

Input: BS location, user location, sensing range R, number of BSs M , number of users N, number of available sub-bands K, maximum number of iterations L.

1: **while** l ¡ L **do**

2: For fixed $\mathbf{p}^{(l)}$ and user association scheme, update the optimal sub-band allocation scheme $\mathbf{w}^{(l+1)}$ based on Algorithm 1.

3: For fixed $\mathbf{p}^{(l)}$ and $\mathbf{w}^{(l+1)}$, update $\mathbf{u}^{(l+1)}$ by solving the problem (17) to achieve load balance.

4: For fixed $\mathbf{u}^{(l+1)}$ and given $\mathbf{w}^{(l+1)}$, optimize transmission power $\mathbf{p}^{(l+1)}$ by solving the problem (18).

5: $l = l + 1$.

6: **end while**

Output: $\mathbf{w}^*$, $\mathbf{u}^*$, $\mathbf{p}^*$.

4.4 Overall algorithm

Based on the aforementioned algorithms, we present the overall algorithm for solving the problem (13) in Algorithm 2. Specifically, we update sub-band allocation $\mathbf{w}$, user association $\mathbf{u}$ and transmission power $\mathbf{p}$ by solving the sub-problem (15), (17, 18) and (21), respectively. By iteratively updating the three variables in an alternative manner, the solution to the problem (13) can be obtained.

5 Simulation results and discussion

In this section, we verify the effectiveness of the proposed algorithms through numerical results. We assume that BSs are uniformly located in a 2-dimension area of $1.5 * 1.5$ km, while the users are randomly distributed in this area. Figure 2 shows an example of the sub-band allocation and user association results obtained by Algorithm 2, where the BSs marked with the same color share the same sub-bands, and the users are served by the associated BSs. Simulation parameters are listed in Table 1.

As far as we know, there have been no existing works studying the problem considered in this paper. Therefore, to show the superiority of the algorithms adopted to solve the three sub-problems, we select the following four benchmark schemes for performance comparison:

(1) Random channel allocation with user association (UA) and transmission power control (TPC), denoted as "Rand+UA+TPC".
(2) Fixed power, in which we set BSs working at maximum power, with GGSA proposed and UA, denoted as "GGSA+UA+FP".
(3) Power control for cooperative ISAC Networks in [21], with GGSA proposed and UA, denoted as "GGSA+UA+[21]".
(4) A low-complexity branch-and-bound algorithm channel allocation [16], where the initial solution also comes from the greedy algorithm, with UA and TPC, denoted as "[16]+UA+TPC".

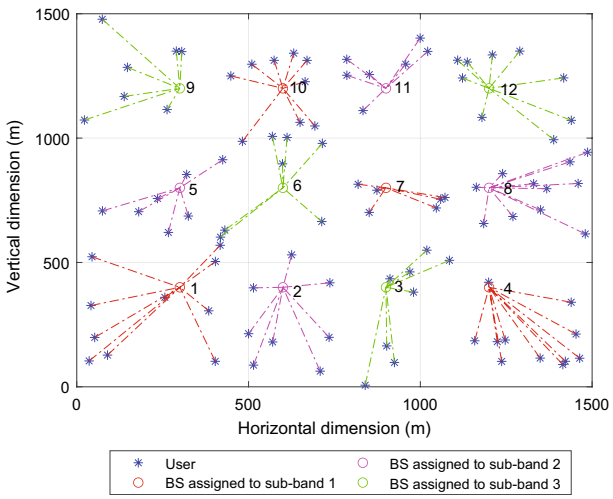

Fig. 2 Simulation diagram with an example of sub-band allocation and user association result ($K = 3$)

Table 1 Simulation parameters

Parameter	Items	Value
Number of BSs	M	12
Number of users	N	100
Number of sub-band	K	{3, 4}
Bandwidth	B	100 MHz
Transmission power	p	1–10 W
Sensing range of each BS	R	500 m
RCS	ψ	30 dBsm
Maximum iteration number	L_{iter}	5
Cross-correlation gain	χ	30 dB
Direct interference suppression gain	β	− 18 dB
SNR	$2p/\sigma^2$	10 dB
Subcarrier spacing	Δf	60 kHz
IFFT size	L	2048

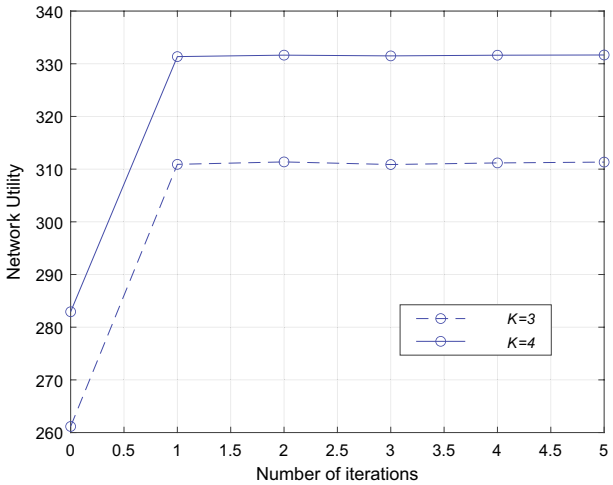

Fig. 3 Network utility versus iteration numbers

Specifically, for sub-band allocation, we compare the performance of Algorithm 2 with scheme (1) and scheme (4). For transmission power, scheme (2) and scheme (3) is set as benchmarks to illustrate the system performance improvement by the proposed transmission power control.

To begin with, we show the convergence of Algorithm 2 in Fig. 3. The network utility at iteration 0 corresponds to "Rand+UA+TPC". It shows that the network utility achieved with the proposed Algorithm 2 increases quickly, and converges (the variation does not exceed 1%) after the first iteration.

In Fig. 4a, we present network utility achieved by different approaches under different sensing SINR thresholds. It can be seen that the network utility under all schemes increases with the number of available sub-bands. By using the proposed Algorithm 2 and the "[16]+UA+TPC" scheme, the network utility is improved compared with the "Rand+UA+TPC","GGSA+UA+FP" and "GGSA+UA+[21]" scheme.

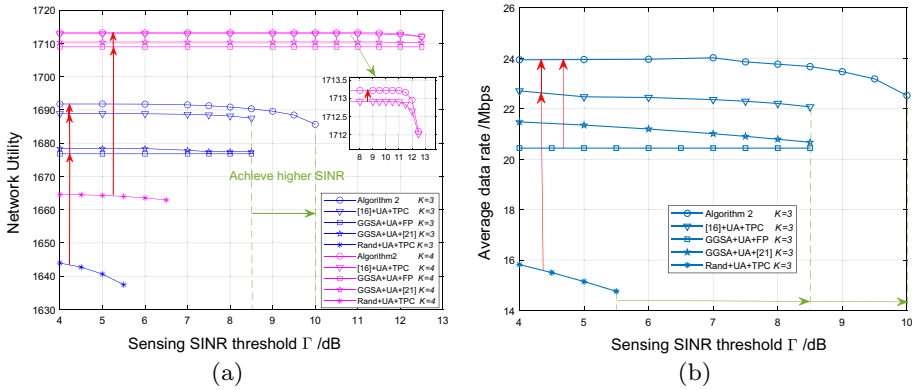

Fig. 4 **a** Network utility versus sensing SINR threshold. **b** Average data rate versus sensing SINR threshold

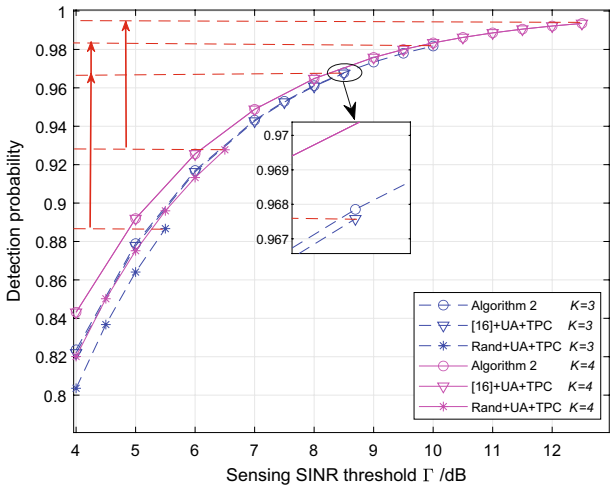

Fig. 5 Detection probability versus sensing SINR threshold

In particular, Algorithm 2 improves the network efficiency slightly higher than the "[16]+UA+TPC", which verifies the effectiveness of the proposed GGSA. In addition, with fewer sub-bands allocable, the proposed Algorithm 2 improves the network utility more significantly than the "[16]+UA+TPC" scheme. Still, it has a feasible solution in a larger sensing SINR threshold. Compared with the "GGSA+UA+FP" and "GGSA+UA+[21]" scheme, the network utility increases under the proposed Algorithm 2 for both $K = 3$ and $K = 4$, which verifies the effectiveness of the proposed TPC algorithm. We also show the average data rate under different sensing SINR thresholds in Fig. 4b. Similarly, the proposed Algorithm 2 achieves best trade-off between the average data rate and achievable sensing SINR.

Figure 5 depicts the detection probability [28] of three schemes under different sensing SINR thresholds. As Fig. 5 shows, with the sensing SINR threshold increasing, the detection probability also increases. For the same scheme, the detection probability of '$K = 4$' is higher than that of '$K = 3$'. The proposed Algorithm 2 and "[16]+UA+TPC" scheme can reach a larger sensing threshold than the other schemes, and also have higher detection probability at the same achievable SINR

threshold. With fewer allocable sub-bands, the proposed Algorithm 2 shows the best performance.

From Figs. 4 and 5, it can be observed that there exists a trade-off between communication and sensing performances. For the "Rand+UA+TPC" scheme, with the increase of sensing SINR threshold, the network utility and average data rate show downward trends. By using Algorithm 2 and the"[16]+UA+TPC" scheme, the network utility can remain stable within a certain range of the singing SINR threshold. Nevertheless, when SINR is greater than a certain value, the network utility will also decline. On the other hand, the detection probability, increases with the increase of SINR for all cases, which shows the trade-off between communication and sensing performances. In what follows, we take the case of $K = 3$ as an example to illustrate the above trade-off.

In Fig. 6, we plot the cumulative distribution function (CDF) curves of transmission power based on 100 simulation results. Since the distribution of BSs is symmetrical, we select four BSs numbered 1, 2, 5, and 6 in Fig. 2 to represent the four types of BSs, namely, edge, general case 1, general case 2, and center. As shown in Fig. 6, when $\Gamma = 4$ dB, the power of the BS 6 in the center is lower than that of BS 1, BS 2, and BS 5. The reason is presented as follows. With a low sensing SINR threshold, more degrees of freedom (DoFs) are reserved to improve the communication performance. Since the central BSs are close to other BSs sharing the same sub-band, which brings about more significant inter-cell interference to the entire network than other BSs, decreasing their transmission power can significantly decrease the inter-cell interference and improve the overall network utility. However, when $\Gamma = 10$ dB, the central BSs require high transmission power to resist the interference from the neighborhood BSs working in the same sub-bands, thereby improving the SINR of echo signals. Therefore, we can see that the power of BS 6 in the center is greater than that of other BSs. In this case, the sensing performance has been improved, while the communication performance is sacrificed and the overall network utility decreases.

In a meantime, we can also see that the BS power distribution is more centralized with $\Gamma = 10$ dB than that with $\Gamma = 4$ dB. Specifically, for $\Gamma = 10$ dB, the power of BS 1, BS 2, and BS 5 all lie in the range of 2.2−2.225 W, while the power of BS 6 is around

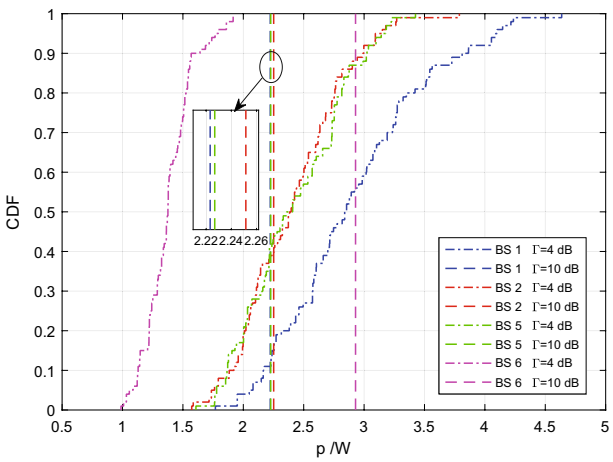

Fig. 6 Power distribution CDF curves ($K = 3$)

2.9 W. As mentioned above, for a high sensing SINR threshold, e.g., $\Gamma = 10$ dB, the central BSs need large power to resist the interference of other BSs. At the same time, they cannot cause too much interference with other BSs. Therefore, the power optimization concentrates their power around a high power so that the power of other BSs is also around a certain value. Under the low sensing SINR constraint, the DoFs for communication optimization is high. The power of each BS can be adjusted with the result of user association to achieve higher network utility. Note that users' locations are random, so user associations vary with each simulation. Therefore, the BSs' power fluctuate in 100 simulations.

6 Conclusion

In this paper, we studied the ISAC design in OFDM-based ISAC-DCN. In this paper, we established the communication and sensing interference models in ISAC-DCN. To address the issue of interference management, we proposed an alternating-optimization-based algorithm for joint sub-band allocation, user association, and transmission power control. To reduce interference and improve the performance of communication and sensing, we proposed a greedy genetic sub-band allocation (GGSA) scheme to reduce total interference. Subsequently, the user association sub-problem was converted to a minimum-weighted bipartite matching problem and solved via the Hungarian algorithm. Moreover, the SCA technique was employed to convert the transmission control sub-problem, which was then solved by GP. Simulation results show that the proposed algorithm significantly improves the network utility and achieves a higher sensing detection probability. Additionally, we analyzed the trade-off between communication and sensing performance in detail. Although this paper focused on the NR systems, it can also be extended to the other ISAC systems, e.g. vehicular network [37], which is left for future work.

Abbreviations

OFDM	Orthogonal frequency division multiplexing
ISAC	Integrated sensing and communication
DCN	Dense cellular network
DL	Downlink
SINR	Signal to interference plus noise ratio
GAGR	Greedy genetic algorithm
SCA	Successive convex approximation
5 G	Fifth-generation
NR	New radio
RS	Reference signal
BS	Base station
DoA	Directions of arrival
FR	Frequency reuse
ICI	Inter-cell interference
UA	User association
TPC	Transmission power control
CDF	Cumulative distribution function
DoF	Degrees of freedom

Author contributions

The authors have contributed jointly to the manuscript. All authors read and approved the final manuscript.

Funding

This work was supported by the National Key R &D Program of China under Grant No. 2021YFB2900200, and the National Natural Science Foundation of China under Grant U20B2039.

Declarations

Competing interests
The authors declare that they have no competing interests.

Received: 22 November 2022 Accepted: 20 June 2023
Published online: 21 July 2023

References

1. F. Liu, Y. Cui, C. Masouros, J. Xu, T.X. Han, Y.C. Eldar, S. Buzzi, Integrated sensing and communications: towards dual-functional wireless networks for 6G and beyond. IEEE J. Sel. Areas Commun. **40**(6), 1728–1767 (2022)
2. 3GPP: NR; Physical channels and modulation. 3rd Generation Partnership Project (3GPP), Technical Specification (TS) 38.211 **9** (2018)
3. L. Hu, Z. Du, G. Xue, Radar-communication integration based on OFDM signal, in *2014 IEEE International Conference on Signal Processing, Communications and Computing (ICSPCC)* (2014), pp. 442–445
4. K. Wu, J.A. Zhang, X. Huang, Y.J. Guo, Joint communications and sensing employing multi-or single-carrier OFDM communication signals: a tutorial on sensing methods, recent progress and a novel design. Sensors **22**(4), 1613–1635 (2022)
5. Y. Cui, X. Jing, J. Mu, Integrated sensing and communications via 5G NR waveform: performance analysis, in *ICASSP 2022—2022 IEEE International Conference on Acoustics, Speech and Signal Processing (ICASSP)* (2022), pp. 8747–8751
6. Q. Zhao, S. Li, A. Tang, X. Wang, Energy-efficient reference signal optimization for 5G V2X joint communication and sensing, in *ICC 2022-IEEE International Conference on Communications* (2022), pp. 1040–1045
7. P. Samczyński, K. Abratkiewicz, M. Płotka, T.P. Zieliński, L. Pucci, E. Paolini, A. Giorgetti, 5G network-based passive radar. IEEE J. Sel. Areas Commun. **60**, 1–9 (2021)
8. L. Pucci, E. Paolini, A. Giorgetti, System-level analysis of joint sensing and communication based on 5G new radio. IEEE J. Sel. Areas Commun. **40**(7), 2043–2055 (2022)
9. Q. Shi, L. Liu, S. Zhang, S. Cui, Device-free sensing in OFDM cellular network. IEEE J. Sel. Areas Commun. **40**(6), 1838–1853 (2022)
10. S. Shi, Z. Cheng, L. Wu, Z. He, B. Shankar, Distributed 5G NR-based integrated sensing and communication systems: frame structure and performance analysis, in *2022 30th European Signal Processing Conference (EUSIPCO)* (2022), pp. 1062–1066
11. N. Bhushan, J. Li, D. Malladi, R. Gilmore, D. Brenner, A. Damnjanovic, R.T. Sukhavasi, C. Patel, S. Geirhofer, Network densification: the dominant theme for wireless evolution into 5G. IEEE Commun. Mag. **52**(2), 82–89 (2014)
12. I. Katzela, M. Naghshineh, Channel assignment schemes for cellular mobile telecommunication systems: a comprehensive survey. IEEE Pers. Commun. **3**(3), 10–31 (1996)
13. F. Luna, C. Blum, E. Alba, A.J. Nebro, Aco vs eas for solving a real-world frequency assignment problem in GSM networks, in *Proceedings of the 9th Annual Conference on Genetic and Evolutionary Computation* (2007), pp. 94–101
14. M. da Silva Maximiano, M.A. Vega-Rodríguez, J.A. Gómez-Pulido, J.M. Sánchez-Pérez, Analysis of parameter settings for differential evolution algorithm to solve a real-world frequency assignment problem in GSM networks, in *2008 The Second International Conference on Advanced Engineering Computing and Applications in Sciences* (2008), pp. 77–82
15. G. Li, H. Liu, Downlink radio resource allocation for multi-cell OFDMA system. IEEE Trans. Wirel. Commun. **5**(12), 3451–3459 (2006)
16. X. Wang, Z. Fei, J. Huang, J.A. Zhang, J. Yuan, Joint resource allocation and power control for radar interference mitigation in multi-UAV networks. Sci. China Inf. Sci. **64**(8), 1–13 (2021)
17. H.T. Long, R. Cai, X.J. Li, P.H.J. Chong, Poster: performance comparison of various: frequency reuse and power masking schemes in 4G ofdma downlink transmissions, in *9th International Conference on Communications and Networking in China* (2014), pp. 682–683
18. K. Lee, O. Jo, D.-H. Cho, Cooperative resource allocation for guaranteeing intercell fairness in femtocell networks. IEEE Commun. Lett. **15**(2), 214–216 (2011)
19. K. Son, S. Chong, G. De Veciana, Dynamic association for load balancing and interference avoidance in multi-cell networks. IEEE Trans. Wirel. Commun. **8**(7), 3566–3576 (2009)
20. B. Post, S. Borst, H. Van Den Berg, Dynamic frequency reuse in dense cellular networks, in *2019 International Symposium on Modeling and Optimization in Mobile, Ad Hoc, and Wireless Networks (WiOPT)* (2019), pp. 1–8
21. M. Liu, M. Yang, H. Li, K. Zeng, Z. Zhang, A. Nallanathan, G. Wang, L. Hanzo, Performance analysis and power allocation for cooperative ISAC networks. IEEE Internet Things J. **10**(7), 6336–6351 (2023)
22. Q. Ye, B. Rong, Y. Chen, M. Al-Shalash, C. Caramanis, J.G. Andrews, User association for load balancing in heterogeneous cellular networks. IEEE Trans. Wirel. Commun. **12**(6), 2706–2716 (2013)
23. S.U. Pillai, H.S. Oh, D.C. Youla, J.R. Guerci, Optimal transmit-receiver design in the presence of signal-dependent interference and channel noise. IEEE Trans. Inf. Theory **46**(2), 577–584 (2000)
24. S. Han, C. Yang, P. Chen, Full duplex-assisted intercell interference cancellation in heterogeneous networks. IEEE Trans. Commun. **63**(12), 5218–5234 (2015)
25. C. Sturm, W. Wiesbeck, Waveform design and signal processing aspects for fusion of wireless communications and radar sensing. Proc. IEEE **99**(7), 1236–1259 (2011)
26. C. Li, S. De Bast, Y. Miao, E. Tanghe, S. Pollin, W. Joseph, Contact-free multitarget tracking using distributed massive mimo-ofdm communication system: prototype and analysis. IEEE Internet Things J. **10**(10), 9220–9233 (2023)
27. F. Colone, D. O'hagan, P. Lombardo, C. Baker, A multistage processing algorithm for disturbance removal and target detection in passive bistatic radar. IEEE Trans. Aerosp. Electron. Syst. **45**(2), 698–722 (2009)

28. A. Khawar, A. Abdelhadi, C. Clancy, Target detection performance of spectrum sharing MIMO radars. IEEE Sens. J. **15**(9), 4928–4940 (2015)
29. J. Xu, C. Guo, J. Yang, Interference-aware greedy channel assignment in multi-radio multi-channel wmn, in *2016 25th Wireless and Optical Communication Conference (WOCC)* (2016), pp. 1–4
30. J.J. Grefenstette, Optimization of control parameters for genetic algorithms. IEEE Trans. Syst. Man Cybern. **16**(1), 122–128 (1986)
31. K. Wang, W. Shang, M. Liu, W. Lin, H. Fu, A greedy and genetic fusion algorithm for solving course timetabling problem, in *2018 IEEE/ACIS 17th International Conference on Computer and Information Science (ICIS)* (2018), pp. 344–349
32. N. Prasad, M. Arslan, S. Rangarajan, Exploiting cell dormancy and load balancing in LTE hetnets: optimizing the proportional fairness utility. IEEE Trans. Commun. **62**(10), 3706–3722 (2014)
33. T. Kim, M. Dong, An iterative Hungarian method to joint relay selection and resource allocation for d2d communications. IEEE Wirel. Commun. Lett. **3**(6), 625–628 (2014)
34. C. Bin, L. Xiaohui et al., User association in heterogeneous cellular networks via the Hungarian method. J. Univ. Electron. Sci. Technol. China **46**(2), 346–351 (2017)
35. D.P. Palomar, M. Chiang, Alternative decompositions and distributed algorithms for network utility maximization, in *GLOBECOM'05. IEEE Global Telecommunications Conference, 2005* (2005), p. 6
36. X. Wang, Z. Fei, J.A. Zhang, J. Huang, J. Yuan, Constrained utility maximization in dual-functional radar-communication multi-uav networks. IEEE Trans. Commun. **69**(4), 2660–2672 (2021)
37. Q. Cui, X. Hu, W. Ni, X. Tao, P. Zhang, T. Chen, K.-C. Chen, M. Haenggi, Vehicular mobility patterns and their applications to internet-of-vehicles: a comprehensive survey. Sci. China Inf. Sci. **65**(11), 1–42 (2022)

Publisher's Note